Monthly Notices of the ROYAL ASTRONOMICAL SOCIETY

MNRAS **466,** 3206–3216 (2017) doi:10.1093/mnras/stw3289
Advance Access publication 2016 December 17

The VMC survey – XXIII. Model fitting of light and radial velocity curves of Small Magellanic Cloud classical Cepheids

M. Marconi,[1⋆] R. Molinaro,[1⋆] V. Ripepi,[1⋆] M.-R. L. Cioni,[2,3] G. Clementini,[4] M. I. Moretti,[1] F. Ragosta,[1] R. de Grijs,[5,6] M. A. T. Groenewegen[7] and V. D. Ivanov[8,9]

[1]*INAF-Osservatorio Astronomico di Capodimonte, Salita Moiariello, 16, I-80131 Napoli, Italy*
[2]*Leibnitz-Institut für Astrophysik Potsdam, An der Sternwarte 16, D-14482 Potsdam, Germany*
[3]*University of Hertfordshire, Physics Astronomy and Mathematics, College Lane, Hatfield AL10 9AB, UK*
[4]*INAF – Osservatorio Astronomico di Bologna, Via Ranzani 1, I-40127 Bologna, Italy*
[5]*Kavli Institute for Astronomy & Astrophysics and Department of Astronomy, Peking University, Yi He Yuan Lu 5, Hai Dian District, Beijing 100871, China*
[6]*International Space Science Institute–Beijing, 1 Nanertiao, Zhongguancun, Hai Dian District, Beijing 100190, China*
[7]*Koninklijke Sterrenwacht van België, Ringlaan 3, B-1180 Brussels, Belgium*
[8]*European Southern Observatory, Ave. Alonso de Córdova 3107, Vitacura, Santiago, Chile*
[9]*European Southern Observatory, Karl-Schwarzschild-Strasse 2, D-85748 Garching bei München, Germany*

Accepted 2016 December 14. Received 2016 December 14; in original form 2016 October 21

ABSTRACT

We present the results of the χ^2 minimization model fitting technique applied to optical and near-infrared photometric and radial velocity data for a sample of nine fundamental and three first overtone classical Cepheids in the Small Magellanic Cloud (SMC). The near-infrared photometry (*JK* filters) was obtained by the European Southern Observatory (ESO) public survey 'VISTA near-infrared *Y*, *J*, K_s survey of the Magellanic Clouds system' (VMC). For each pulsator, isoperiodic model sequences have been computed by adopting a non-linear convective hydrodynamical code in order to reproduce the multifilter light and (when available) radial velocity curve amplitudes and morphological details. The inferred individual distances provide an intrinsic mean value for the SMC distance modulus of 19.01 mag and a standard deviation of 0.08 mag, in agreement with the literature. Moreover, the intrinsic masses and luminosities of the best-fitting model show that all these pulsators are brighter than the canonical evolutionary mass–luminosity relation (MLR), suggesting a significant efficiency of core overshooting and/or mass-loss. Assuming that the inferred deviation from the canonical MLR is only due to mass-loss, we derive the expected distribution of percentage mass-loss as a function of both the pulsation period and the canonical stellar mass. Finally, a good agreement is found between the predicted mean radii and current period–radius (PR) relations in the SMC available in the literature. The results of this investigation support the predictive capabilities of the adopted theoretical scenario and pave the way for the application to other extensive data bases at various chemical compositions, including the VMC Large Magellanic Cloud pulsators and Galactic Cepheids with *Gaia* parallaxes.

Key words: stars: distances – stars: oscillations – stars: variables: Cepheids – Magellanic Clouds.

1 INTRODUCTION

Classical Cepheids (CCs) are widely adopted as primary distance indicators to calibrate the extragalactic distance scale. Indeed, several secondary distance indicators, which are able to directly constrain the Hubble constant, rely on Cepheid period–luminosity (PL) and period–luminosity–colour (PLC) relations (see e.g. Freedman et al. 2001; Saha et al. 2001; Riess et al. 2016, and references therein). From the evolutionary point of view, Cepheids are intermediate-mass stars during the central helium burning phase (see e.g. Bono et al. 2000; Valle et al. 2009, and references therein), crossing the instability strip as they move bluewards in the Hertzprung–Russell (HR) diagram (*blue loop* excursion) at constant luminosity for each given mass. Thus, stellar evolution predicts a mass–luminosity relation (MLR) for CCs. This MLR, combined with the period–density relation and the Stefan Boltzmann law,

⋆ E-mail: marcella@na.astro.it (MM); rmolinaro75@gmail.com (RM); vincenzo.ripepi@oacn.inaf.it (VR)

produces a PLC relation, holding for each individual Cepheid (see e.g. Bono et al. 1999b; Marconi, Musella & Fiorentino 2005; Marconi 2009, and references therein). Then, projecting the PLC on to the PL plane gives the PL relation (see e.g. Madore & Freedman 1991; Bono et al. 1999b; Marconi 2009). On this basis, the investigation of Cepheid pulsation properties is also crucial for providing independent constraints on the MLR. Several authors have discussed the uncertainties related to this MLR as due to core overshooting and/or mass-loss (see e.g. Chiosi, Wood & Capitanio 1993; Wood Arnold, Sebo 1997; Bono et al. 1999b; Caputo et al. 2005; Keller & Wood 2006; Marconi et al. 2013b; Musella et al. 2016, and references therein), often related to the so called *mass discrepancy* problem (see e.g. Marconi et al. 2013b, and references therein, for details), first suggested by Stobie (1969) and Christy (1970). These authors noticed that the Cepheid *evolutionary* masses based on the application of theoretical isochrones to observations were larger than the *pulsational* ones, e.g. based on period–mass–radius relations (Fricke, Stobie & Strittmatter 1971; Bono et al. 2001). One of the methods that has been recently adopted by our team to address the mass discrepancy problem is the so called model fitting of multifilter light, radial velocity and radius curves (see e.g. Keller & Wood 2006; Natale, Marconi & Bono 2008; Marconi et al. 2013a,b, and references therein), through the direct comparison of the observed and predicted variations along a pulsation cycle, the latter based on non-linear convective pulsation models (see Bono, Castellani & Marconi 2000, 2002; Marconi et al. 2013b, for details). In particular, beyond the application to the prototype δ Cephei (see Natale et al. 2008), three papers have been devoted by our team to the model fitting of variations for Cepheids in the Large Magellanic Cloud (LMC).

(i) In Bono et al. (2002), we fitted the *V*-, *I*-band light curves of two LMC bump Cepheids from the OGLE data base (Udalski et al. 1999), with the bump (secondary maximum) along either the decreasing (OGLE 194103, shorter period Cepheid) or the rising (OGLE 56087, longer period Cepheid) branch of the light curve. The adopted non-linear convective pulsation models reproduced the luminosity variation over the entire pulsation cycle if the adopted stellar mass for both Cepheids was roughly 15 per cent smaller than predicted by the evolutionary models, neglecting mass-loss and convective core overshooting. Moreover, the model fitting procedure provided a distance modulus to the LMC of 18.53 ± 0.05 mag. This value was in excellent agreement with the results based on the model fitting technique applied by other teams (see e.g. Keller & Wood 2006, and references therein) to LMC Cepheids from the MACHO (Alcock et al. 1999) data base, as well as with the distance obtained from application of the model fitting technique to RR Lyrae (Marconi & Clementini 2005) or δ Scuti (McNamara, Clementini & Marconi 2007) pulsators.

(ii) In Marconi et al. (2013a), we fitted the multifilter (*U*, *B*, *V*, *I* and *K*) light and radial velocity curves of five Cepheids in NGC 1866, an LMC young massive cluster. Again, the inferred stellar parameters corresponded to an MLR slightly brighter than the canonical one, as an effect of mild overshooting and/or mass-loss, and to individual distances consistent within the uncertainties. The resulting mean distance modulus [18.56 ± 0.03 (stat) ± 0.1 (syst) mag] was found to be in agreement with the literature as well as with the previous model fitting applications.

(iii) In Marconi et al. (2013b), we fitted the light and radial velocity curves of the LMC Cepheid OGLE-LMC-CEP-0227 belonging to a detached double-lined eclipsing binary system, finding, for the best-fitting model, a pulsation mass, a mean effective temperature, a luminosity amplitude and a mean radius in agreement with the empirical estimates. The inferred MLR was again more in agreement with the evolutionary models including a moderate amount of overshooting and/or mass-loss (Cassisi & Salaris 2011; Prada Moroni et al. 2012), the best-fitting chemical composition was more metal-poor than typical LMC Cepheids ($Z = 0.004$ versus 0.008) and slightly helium enhanced ($Y = 0.27$ versus 0.25) and the inferred true distance modulus of the LMC [18.50 ± 0.02 ± 0.10 (syst) mag] was found to be in excellent agreement with similar estimates from independent methods in the literature.

In this paper, we extend previous analyses to a sample of nine fundamental (F) and three first overtone (FO) CCs in the Small Magellanic Cloud (SMC) that are also targets of the 'VISTA near-infrared YJKs survey of the Magellanic Clouds System' (VMC, P.I.: Cioni; see Cioni et al. 2011).

The organization of the paper is the following. In Section 1, we discuss the sample selection with a brief outline of the VMC survey. In Section 2, we recall the main steps of the adopted model fitting technique and in Section 3, its application to the selected SMC Cepheids. Section 4 deals with the implications of the model fitting results for what concerns the MLR, the period-radius (PR), the PL and the Wesenheit relations. The final section includes the summary and some perspectives.

2 SELECTION OF THE SAMPLE

The selected sample of CCs includes nine F and three FO pulsators with optical photometry from the OGLE III data base (Soszyński et al. 2010) and NIR photometry from the VMC survey (Cioni et al. 2011; Ripepi et al. 2016). For Harvard Variable (HV) stars, we also used *V*, *I*, *J*, *K* data from Storm et al. (2004). We transformed the *J*- and *K*-band data by these authors from the California Institute of Technology (CIT) photometric system to the VISTA system. To this aim, we used equations by Carpenter (2001) to pass from CIT to 2MASS system and then we transformed 2MASS data to VISTA by using the equations provided by the Cambridge Astronomy Survey Unit (CASU),[1] (see also Ripepi et al. 2016).

VMC covers the entire Magellanic system with deep NIR (*Y*, *J*, K_s filters) VIRCAM (VISTA InfraRed Camera; Dalton et al. 2006) photometry on the European Southern Observatory (ESO)/VISTA telescope (Emerson et al. 2006). This survey aims at deriving the star formation history and its spatial variation and an accurate 3D map of the Magellanic system by using pulsating stars as distance indicators and tracers of stellar populations (see e.g. Ripepi et al. 2012a,b, 2014, 2015; Moretti et al. 2014; Muraveva et al. 2015, and references therein). In particular, the VMC SMC Cepheids have been presented and discussed by Ripepi et al. (2016) and Moretti et al. (2016). The average number of phase points are 5.7, 6.3 and 16.7 in *Y*, *J*, K_s, respectively (see Ripepi et al. 2016, for details).

The properties of the selected SMC Cepheids are reported in the first six columns of Table 1. The first two columns report the identification and the pulsation mode, whereas the third and fourth columns provide the period and epoch information. The available data are reported in the fifth column (only photometry or photometry and radial velocity), while the intensity mean magnitude in the *V* band, derived from the best-fitting models, is shown in column six.

The radial velocity data for the three last variables in Table 1 are taken from Storm et al. (2004). They are derived with the cross-correlation method (see Storm et al. 2004, for details).

[1] http://www.astro.caltech.edu/jmc/2mass/v3/transformations/

Table 1. Properties of the selected SMC Cepheids.

ID	Mode	P (d)	Epoch (HJD)	Data	$<V>$ (mag)	$T_{\rm eff}$ (K)	$\log(L/L_\odot)$ (dex)	$M/M_\odot$	$R/R_\odot$	$\mu_0 \pm (\delta\mu_0)_{\rm rms}$ (mag)	$(\delta\mu_0)_{\rm grid}$	p	$(\delta p)_{\rm grid}$ (km s^{-1})	$\gamma \pm (\delta\gamma)_{\rm rms}$ (km s^{-1})
OGLE 0646	FO	1.278 1746	50 621.243 75	phot.	17.207	6425	2.78	3.6	19.9	19.01 ± 0.06	(−0.02; 0.06)			
OGLE 1021	FO	1.600 6633	50 621.421 65	phot.	17.171	6350	2.83	3.0	21.6	18.94 ± 0.03	(−0.02; 0.02)			
OGLE 2306	FO	1.606 3795	50 621.503 67	phot.	17.091	6450	2.86	3.0	21.6	18.93 ± 0.06	(−0.02; 0.02)			
OGLE 1518	F	2.876 6747	50 465.340 00	phot.	16.676	6160	3.00	3.8	28.1	19.01 ± 0.12	(−0.03; 0.01)			
OGLE 3588	F	5.319 0652	50 619.019 47	phot.	15.681	5975	3.35	5.0	44.4	19.00 ± 0.10	(−0.01; 0.03)			
OGLE 3533	F	7.989 6097	52 102.058 14	phot.	15.163	5900	3.50	4.6	54.0	18.97 ± 0.04	(−0.02; 0.02)			
OGLE 1165	F	10.309 0126	50 612.863 64	phot.	15.911	5700	3.66	6.0	69.4	19.23 ± 0.06	(−0.01; 0.03)			
HV 1345	F	13.4784	47 496.0	phot./$v_{\rm rad}$	14.765	5325	3.60	5.0	74.2	18.97 ± 0.14	(−0.02; 0.02)	1.38	(−0.05; 0.05)	105.8 ± 7.3
HV 1335	F	14.3816	50 610.6	phot./$v_{\rm rad}$	14.809	5325	3.66	5.4	79.6	19.10 ± 0.16	(−0.01; 0.02)	1.40	(−0.05; 0.01)	154.1 ± 4.9
OGLE 2841	F	14.712 884	50 616.271 51	phot.	14.955	5350	3.73	5.9	86.4	19.03 ± 0.08	(−0.02; 0.01)			
HV 822	F	16.7421	47 485.9	phot./$v_{\rm rad}$	14.538	5320	3.77	5.9	90.6	18.98 ± 0.12	(−0.03; 0.04)	1.16	(−0.03; 0.01)	99.0 ± 3.1
OGLE 2470	F	42.746 8803	52 079.012 57	phot.	13.242	5400	4.41	9.8	183.6	18.97 ± 0.11	(−0.04; 0.05)			

The selected 12 stars were chosen in order to span different periods, amplitudes and morphologies of the observed light curves from Ripepi et al. (2016) data base. Even if they do not represent the entire sample, their properties allow us to test the predictive capability of the model fitting technique on a variety of observed Cepheid properties in the same stellar system. We note that a statistically significant extension of the selected target number would be extremely time-consuming, given the accuracy of the fitting procedure. We also note that the selected CCs are well distributed across the SMC body (see Fig. 1).

3 THE MODEL FITTING TECHNIQUE

The fitting technique, applied to find the best model reproducing the observations, is the same as that adopted in Marconi et al. (2013a). The photometric curves of the models have been phased in order to find the V band maximum of light at phase zero. Afterwards, for each modelled photometric band, we estimated the magnitude shift, δM, which provides the best match with the observed light curves. Specifically, indicating with m and $M_{\rm model}$ the observed apparent magnitude and the model absolute magnitude, respectively, we minimized the following χ^2 function:

$$\chi^2 = \sum_{i=1}^{N_{\rm bands}} \sum_{j=1}^{N_{\rm points}} \left[m_j^i - \left(M_{\rm model}^i(\phi_j^i + \delta\phi^i) + \delta M^i \right) \right]^2 , \quad (1)$$

where the two sums are performed over the number of bands, $N_{\rm bands}$, and the number of measures, $N_{\rm points}$. To estimate the value of the model magnitude at the same phase of the observations, we have used a smooth spline interpolation. The fitted parameters are $\delta\phi$, which represents possible small residual ($\sim\pm0.1$) phase shifts between model and data, and δM^i, which represents the distance modulus in the ith photometric band.

For the three Cepheids with radial velocity observations, we transformed the modelled pulsational velocity into radial velocity by using the equation $v^{\rm radial} = (-1/p)v^{\rm model}$, where p is the projection factor. In this case, the χ^2 function assumes the form:

$$\chi^2 = \sum_{j=1}^{N_{\rm points}} \left[v_j - \left(-\frac{1}{p} v^{\rm model} \left(\phi_j + \delta\phi \right) + \gamma \right) \right]^2 , \quad (2)$$

where v is the observed radial velocity and γ is the barycentric velocity. As in the case of the photometry, we calculated the pulsational velocity at the phase of the observed data by using a smooth spline interpolation. In this case, the fitted parameters are the barycentric velocity and the projection factor as well as the phase shift $\delta\phi$ between data and models.

We notice that the uncertainty affecting the p factor is still the main source of systematic errors in the various versions of the Baade–Wesselink method and its value and possible period dependence are lively debated in the literature (see e.g. Molinaro et al. 2011; Marconi et al. 2013a, and references therein). The model fitting of radial velocity curves represents an independent tool to constrain the value of this crucial parameter (see also Natale et al. 2008, and references therein).

For Cepheids with radial velocity data, we combined the χ^2 functions defined above by normalizing the rms of residuals in each band and radial velocity by their corresponding pulsation amplitudes, and then we summed in quadrature to obtain a total normalized rms.

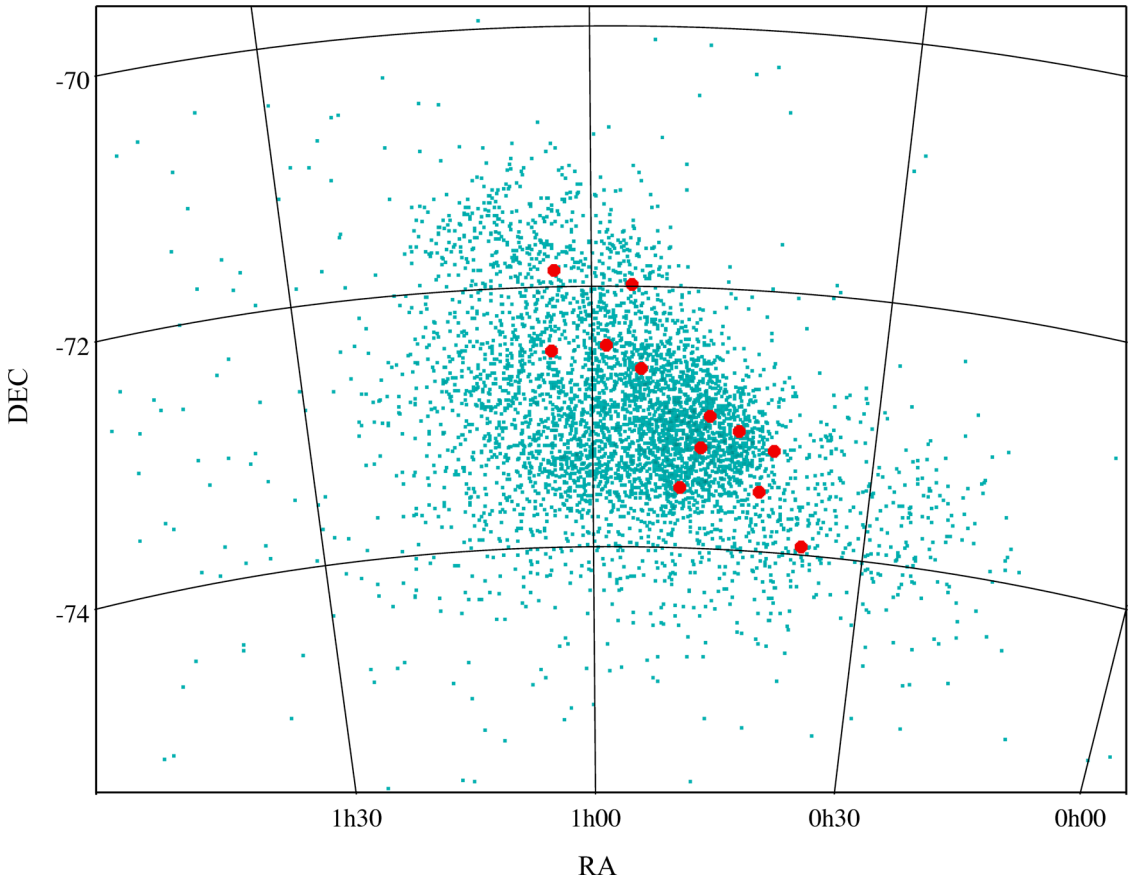

Figure 1. The distribution in right ascension and declination of the selected CCs. The whole SMC data set is shown for comparison.

4 APPLICATION TO THE SELECTED SMC CEPHEIDS

Following a similar strategy to the one adopted in Marconi et al. (2013a,b), we constructed a large set of pulsation models by adopting the typical chemical composition of SMC young stellar population ($Z = 0.004$, $Y = 0.25$; see e.g. Luck et al. 1998; Romaniello et al. 2008), varying the stellar parameters mass, luminosity and effective temperature in order to match the pulsation periods (see Table 1). The output bolometric light curves were converted into observational bands by using static model atmospheres by Castelli, Gratton & Kurucz (1997a,b) and, for the NIR filters, subsequent conversion of Johnson–Cousin magnitudes into the VISTA photometric system, by using the following equations from Ripepi et al. (2016):

$$\begin{aligned} K_S^V &= K^J + 0.007(V-K)^J + 0.03(J-K)^J - 0.038 \\ (V-K_S)^V &= 0.993(V-K)^J - 0.03(J-K)^J + 0.038 \\ (J-K_S)^V &= 0.87(J-K)^J - 0.01. \end{aligned} \quad (3)$$

For each individual pulsator, at the corresponding fixed period, we first assumed a stellar mass and varied the stellar luminosity and effective temperature. For example, in the case of variable HV822 (see Table 1), by applying the χ^2 analysis to the models computed at fixed chemical composition ($Z = 0.004$, $Y = 0.25$) and stellar mass ($M = 7.0\ \mathrm{M}_\odot$), we find that the effective temperature of the best-fitting model is $T_{\rm eff} = 5320 \pm 25$ K (see Figs 2 and 3), corresponding to a luminosity level of $\log L/\mathrm{L}_\odot = 3.84 \pm 0.01$. The uncertainties on the best-fitting intrinsic parameters correspond to the step in mass and effective temperature of the different sets of models. Then, we fixed the effective temperature of the obtained best-fitting solution ($T_{\rm eff} = 5320$ K) and varied the mass and luminosity with a step of 0.1 in $M/\mathrm{M}_\odot$ and of 0.01 dex in $\log L/\mathrm{L}_\odot$ until the best-fitting model is obtained by minimization of the combined photometry and radial velocity χ^2 (see discussion in the previous section and in Marconi et al. 2013a,b). Fig. 4 shows the model fitting of variable HV822 by varying the mass and the luminosity at fixed period and effective temperature. The minimum χ^2 is obtained for $M/\mathrm{M}_\odot = 5.9$ and $\log L/\mathrm{L}_\odot = 3.77$.

Since it is difficult to evaluate by eye the quality of the fit from Figs 3 and 4, we show in Fig. 2 the normalized rms of residuals as a function of the model effective temperature (left-hand panel) and mass (right-hand panel). The plotted rms values in the left-hand panel are those of the models shown in Fig. 3, which are generated by fixing the mass value ($M = 7.0\ \mathrm{M}_\odot$) and varying the effective temperature. As evident from the figure, the best effective temperature is $T_{\rm eff} = 5320$ K. The models plotted in the right-hand panel correspond to those in Fig. 4, obtained by fixing the effective temperature to the best-fitting value and changing the mass. The inferred true distance modulus μ_0, the p factor and the barycentric velocity γ are labelled for each dot.

The same kind of analysis is applied to the other stars listed in Table 1 and the corresponding best-fitting models are shown in Figs 5 and 6.

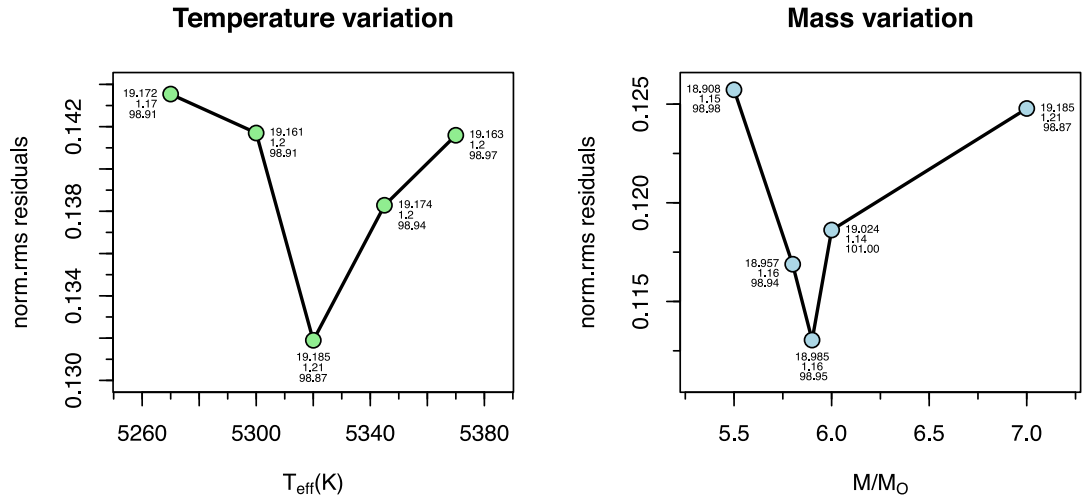

Figure 2. The normalized rms of residuals obtained from the fitting procedure applied to HV822 are shown as a function of the model effective temperature (left-hand panel) and mass (right-hand panel). The inferred true distance modulus μ_0, the p factor and the barycentric velocity γ are labelled for each dot.

We note that, at least for variables HV1335 and HV1345, the decreasing branch of the observed radial velocity curve is not well reproduced by pulsation models. However, the good fit obtained for the *K*-band light curve, in a region of the spectrum where the radial variations dominate over the thermal effects, seems to suggest that the reason of the discrepancy is not to be ascribed to the pulsational computations. On the other hand, we cannot exclude the discrepancy be due to the lack of description of the dynamical structure of the Cepheid atmosphere (Nardetto, private communication; Nardetto et al. 2017). The intrinsic stellar parameters, namely the effective temperature, the luminosity, the mass and the mean radius (see the next section) of the obtained best-fitting models are reported in columns 7–10 of Table 1. We also give an estimate of two different contributions to the error on the fitted parameters: one associated with the step in mass and temperature of the different sets of models, and the other due to the rms of observations around the best-fitting models (see also Marconi et al. 2013b). The final three columns of the same table report the inferred intrinsic distance modulus, p factor and barycentric radial velocity with the associated uncertainties. In the case of HV822, the inferred p factor is lower than the value obtained for HV1335 and HV1345 in spite of the rather similar stellar parameters. Indeed, HV822 has almost the same effective temperature but slightly higher mass and luminosity and lower gravity. To test to what extent this result depends on the photometric information, we also tried to fit the radial velocity curve only and found a best-fitting model with similar stellar parameters (fainter by 0.01 dex and less massive by 0.1 $M_{\odot}$), but a p factor around 1. On this basis, we decided to keep our originally obtained best-fitting model, that correctly takes into account all the available observations. A detailed investigation of the predicted p factor dependence on stellar parameters is beyond the purposes of this paper and will be addressed in a future publication (Molinaro et al., in preparation).

5 IMPLICATIONS OF RESULTS

In this section, we use the results obtained for the intrinsic stellar parameters of the investigated CCs to determine constraints both on the predicted MLR and PR relations as well as on the relations that make CCs powerful standard candles, namely the PL and Wesenheit relations, at least for the SMC chemical composition.

5.1 The MLR

The stellar masses and luminosities of the best-fitting models listed in Table 1 can be plotted in the MLR plane (see Fig. 7) and compared with current predictions for canonical and non-canonical MLRs. The black solid and open symbols are the F and FO best-fitting models listed in Table 1, respectively. Their location in the MLR plane is compared with the evolutionary predictions concerning the canonical (no overshooting, no mass-loss) MLR of Bono et al. (2000) and with the relations obtained by increasing the zero-point of the canonical one by 0.25 dex (dashed line) and 0.5 dex (dotted line) to reproduce the effect of mild and full overshooting, respectively (see e.g. Chiosi et al. 1993; Bono, Marconi & Stellingwerf 1999a for details). According to the points in Fig. 7, the investigated pulsators do not follow a strict MLR, as expected in the case of canonical models or constant overshooting efficiency, but seem to favour a varying overluminosity with respect to the canonical relation. Indeed, most of the Cepheids are located between the mild and full overshooting lines. Even if at this stage we cannot disentangle the role of overshooting and mass-loss in producing the quoted overluminosity, the detected dispersion might indicate a combination of the two non-canonical phenomena. If overshooting was important, and this is a fundamental physics aspect of stellar evolution, for a given mass, one would in principle expect the same amount of overshooting (within small uncertainties). The scatter we find in Fig. 7, seems to imply that another process, e.g. mass-loss, should be important. On the other hand, if only mass-loss was at work, this could be inferred from the predicted deviation of the best-fitting stellar mass from the value corresponding to the canonical MLR. Such a deviation is represented in Fig. 8 as a function of the pulsation period (bottom panel) and of the canonical mass (top panel) for the Cepheids in our sample. We note that the expected mass differences range from less than 2 per cent to almost 30 per cent and are not clearly correlated neither with the pulsation period nor with the stellar mass. The dependence of mass-loss efficiency on the pulsation period is debated in the literature, with *IRAS* data suggesting roughly constant values, and *IUE* spectra indicating a dependence of the mass-loss rate on

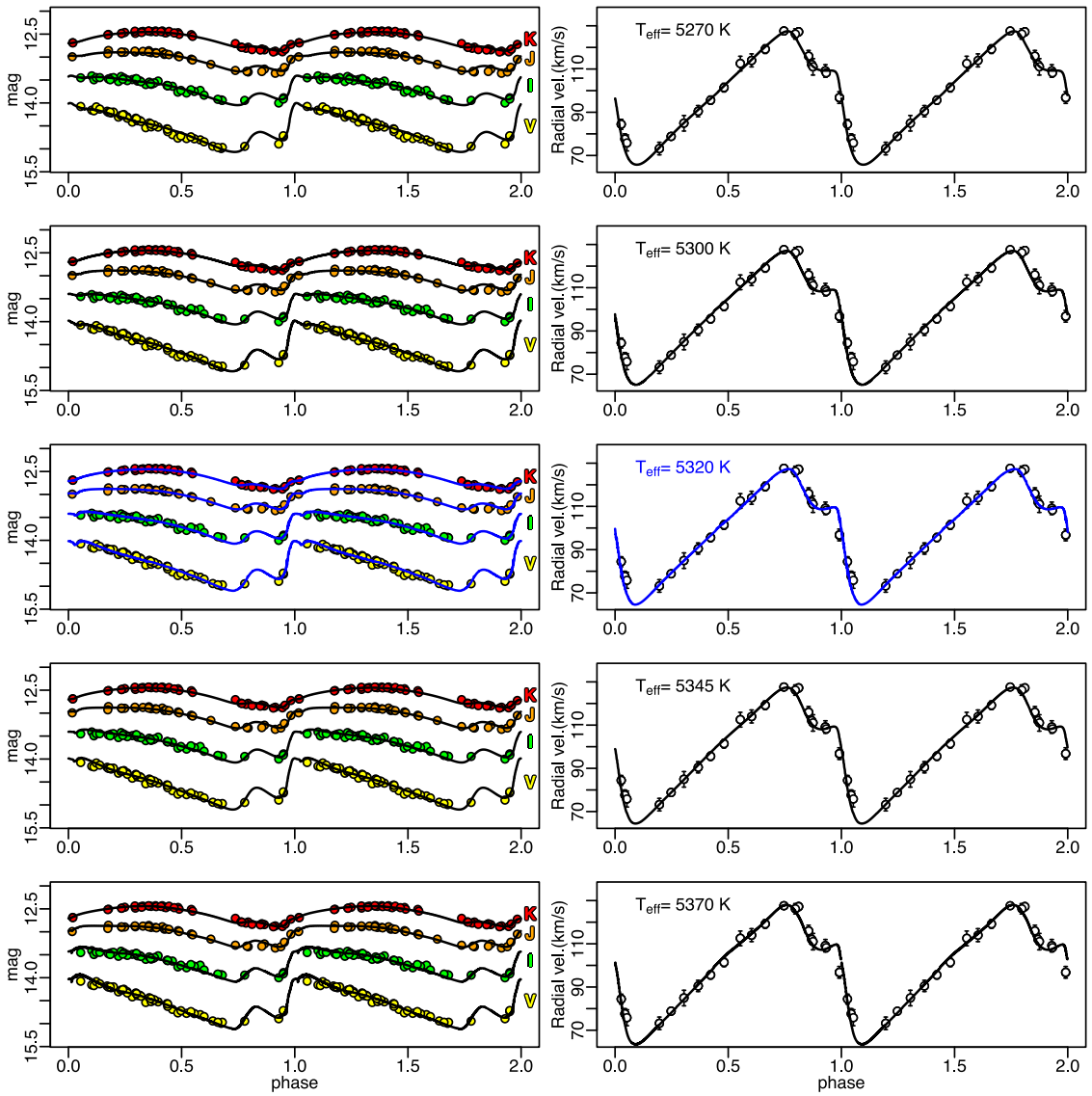

Figure 3. Model fitting procedure followed to estimate the best-fitting effective temperature for the Cepheid HV822. Photometry (left-hand panels) and radial velocity (right-hand panels) are plotted for models with fixed stellar mass value ($M = 7.0\,M_{\odot}$) and varied effective temperature from $T_{\rm eff} = 5270$ to 5370 K. The effective temperature of the best-fitting model (blue lines) is equal to the value that minimizes the χ^2 functions of equations (1) and (2). As the mean error bar for photometry is always <0.02 mag, we do not plot it for clarity reasons.

the pulsation period but without considering possible differences in the evolutionary times (see e.g. Caputo et al. 2005; Neilson & Lester 2008; Neilson et al. 2016, and references therein). In conclusion, our results do not allow us to disentangle between mass-loss and overshooting contributions to the observed overluminosity of the investigated pulsators, leaving the possibility that a combination of the two non-canonical phenomena might be at work.

5.2 The PR relation

The adopted non-linear hydrodynamical code also allows us to model the variation of radius along the pulsation cycle for each pulsation model. Once the radius curve is obtained, we are able to derive the time-averaged mean radius and to correlate it with the corresponding pulsation period. The location of the 11 best-fitting models obtained in the previous section in the period–mean radius diagram is shown in Fig. 9.

In this plot, F and FO best-fitting models are represented by black solid and open circles, respectively; the red symbols correspond to the SMC observed CCs with radii estimated by Storm et al. (2004). The solid line is the theoretical linear regression for the complete sample where the three FO periods have been fundamentalized.[2] Unfortunately, no empirical SMC PR relation has been published in the literature to be compared with our theoretical relation. The dotted line depicts the linear relations derived by Molinaro et al. (2012) on the basis of the CORS Baade–Wesselink method applied to a sample of 11 Cepheids belonging to the young LMC blue populous cluster NGC 1866, while the dashed line is the relation

[2] We considered the period the star would have if it were a F pulsator. This is computed by the linear pulsation code that is adopted to evaluate the radial eigenfunctions and to provide the envelope structure for subsequent non-linear pulsation computations (see Bono et al. 1999a, and references therein)

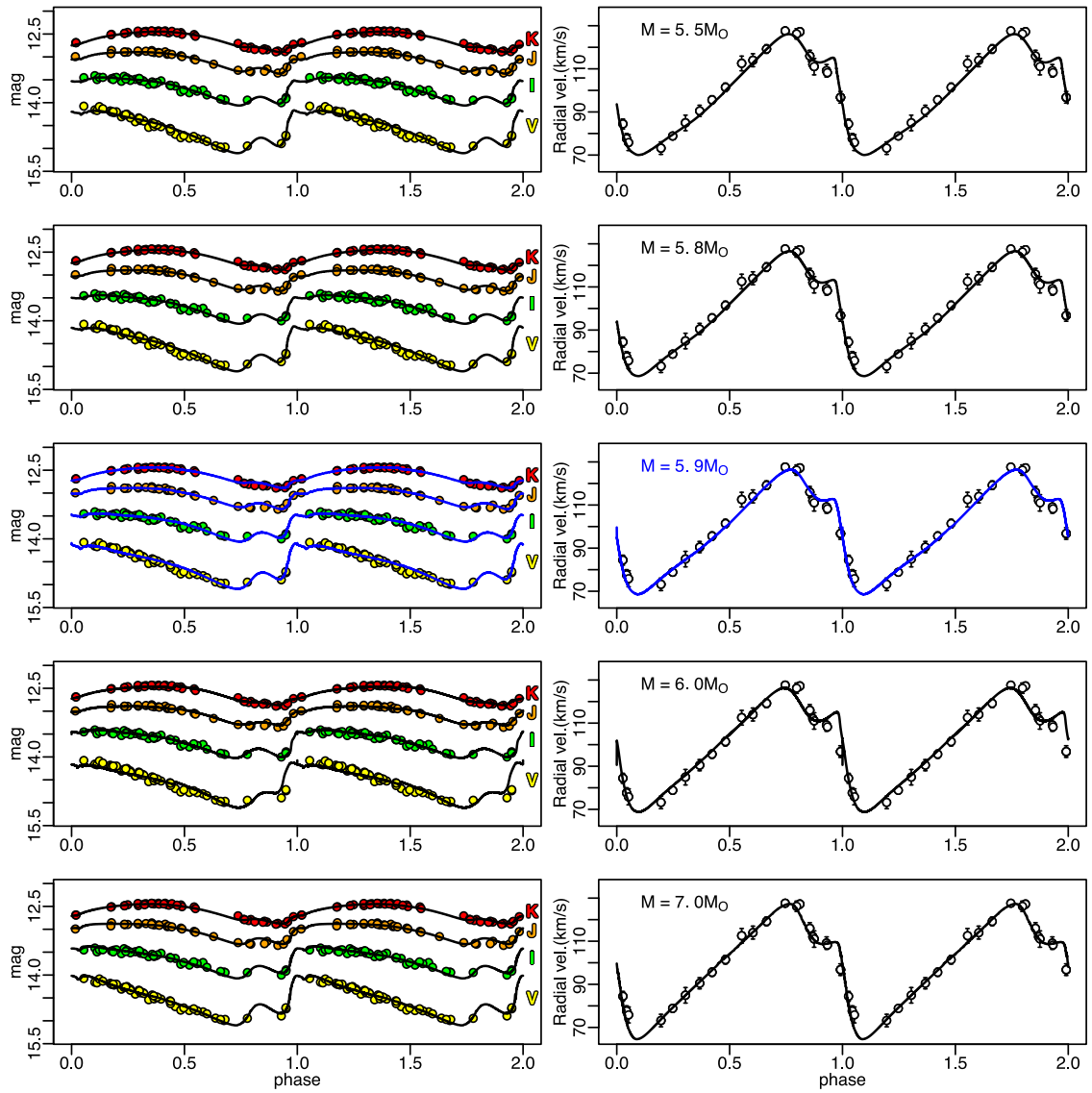

Figure 4. Model fitting procedure followed to estimate the best-fitting mass for the Cepheid HV822. Similarly to Fig. 3, the photometry (left-hand panels) and radial velocity (right-hand panels) are plotted for models with effective temperature equal to the best-fitting value ($T_{\rm eff} = 5320\,K$) and mass value varying from $M = 5.5$ to $7.0\,M_{\odot}$. The mass of the best-fitting model (blue line in plot) is equal to the value that minimizes the χ^2 functions of equations (1) and (2). As the mean error bar for photometry is always <0.02 mag, we do not plot it for clarity reasons.

derived by Gieren et al. (1999) for a sample of both Galactic and Magellanic Cepheids. We note that the predicted PR relation based on the model fitting of SMC Cepheids suggests that at fixed period the radius is smaller for SMC Cepheids than for Galactic and LMC ones. This result was already obtained by Storm et al. (2004) on the basis of the comparison presented in that paper between the radii of SMC and Galactic Cepheids.

5.3 The PL relations

The mean magnitudes of the best-fitting models can be correlated with the corresponding periods to build multifilter PL relations. In Fig. 10, we show the location of both F (red solid circles) and FO (blue open circles) best-fitting models in the *V*-, *I*- and *K*-band magnitude versus period planes. The PL relations recently obtained by the OGLE IV collaboration (Soszyński et al. 2015, S15 in the label) and by the VMC collaboration (Ripepi et al. 2016, R16 in the label) for larger Cepheid samples including our targets are overplotted for the average distance moduli obtained in the various bands by subtracting these relations to the Cepheid absolute magnitudes. As the empirical VMC relations have been corrected for reddening (see Ripepi et al. 2016, for details), their application to the absolute *K*-band magnitudes of our sample directly provides the intrinsic distance modulus μ_0 (see the label).

On the other hand, the difference between the obtained μ_V and μ_I provides and independent estimate of the average colour excess $E(V - I) = 0.14 \pm 0.12$ mag, where the error is the standard deviation. This value is in agreement, within the errors, with the literature estimates (see e.g. Haschke, Grebel & Duffau 2011; Moretti et al. 2016; Ripepi et al. 2016, and references therein). We also note that the theoretical slopes agree quite well with the empirical ones, for both F and FO pulsators. Moreover, the inferred intrinsic

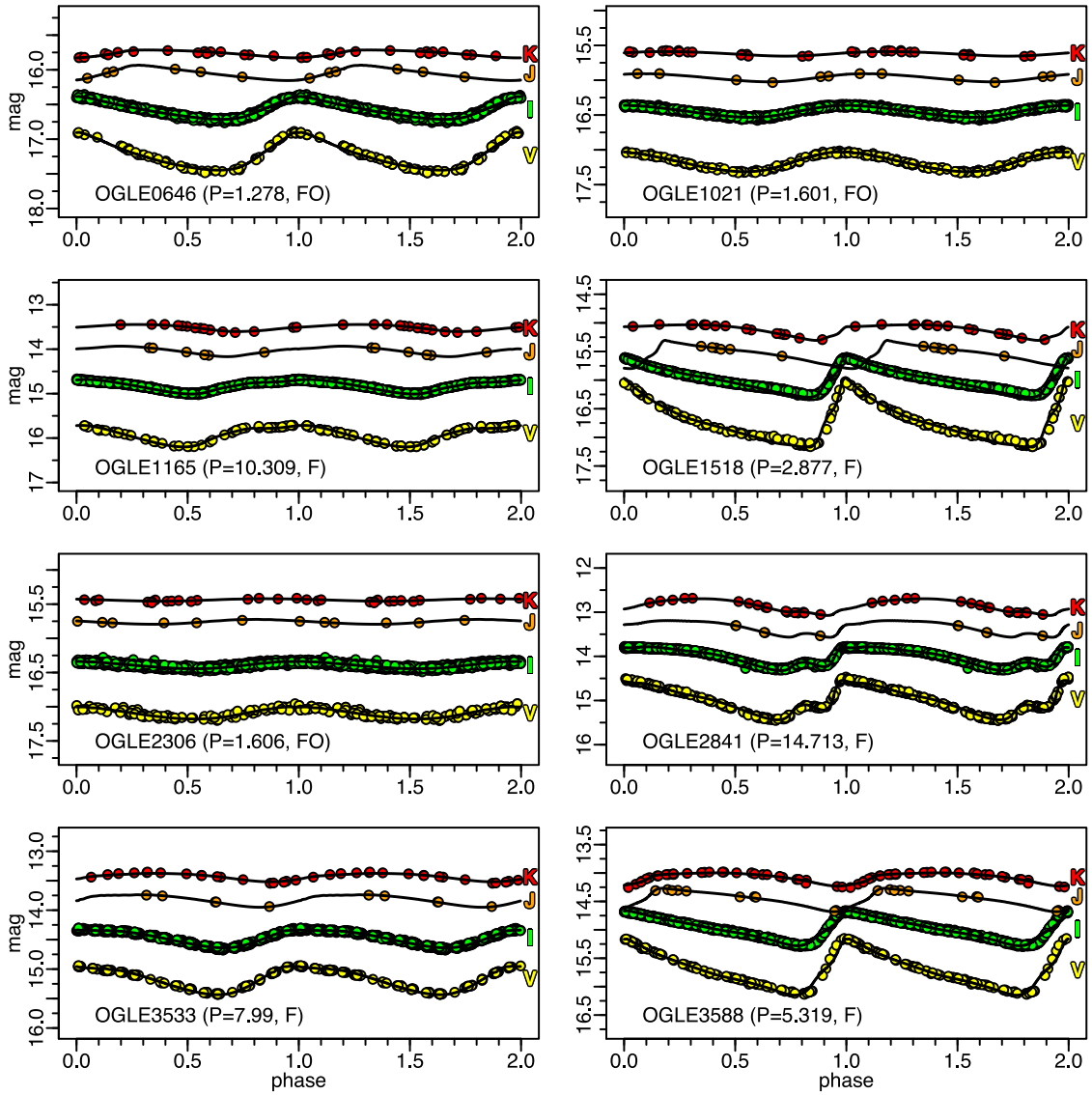

Figure 5. Model fitting of selected SMC Cepheids for which only multifilter light curves are available. The variable identification, pulsation period and mode are labelled in each panel. As the mean error bar is always <0.02 mag, we do not plot them for clarity reasons. The longest period Cepheid OGLE2470 is shown in Fig. 6 for clarity reasons.

mean distance modulus is equal to $\mu_0 = 19.01$ mag and its standard deviation to 0.08 mag, in agreement with the most recent literature values (see de Grijs & Bono 2015; Ripepi et al. 2016, and references therein).

5.4 The Wesenheit relations

Finally, it is interesting to compare the predicted properties of the SMC Cepheids in our sample with currently adopted Wesenheit relations. These are reddening-free PLC relations, obtained by fixing the colour term coefficient to the ratio between total to selective extinction in the considered filters (see e.g. Madore 1982; Caputo, Marconi & Musella 2000; Bono et al. 2010; Fiorentino, Musella & Marconi 2013; Ripepi et al. 2016, and references therein). In particular, to exploit both the optical and the NIR data, we adopt $W(V, I) = I - 1.55 \times (V - I)$ and $W(V, K) = K - 0.13 \times (V - K)$ according to recent prescriptions in the literature (see e.g. Soszyński et al. 2015; Ripepi et al. 2016, and references therein).

As shown in Fig. 11, the models that best reproduce the light curves of the selected SMC Cepheids nicely agree with the empirical SMC Wesenheit relations recently presented by Soszyński et al. (2015) and Ripepi et al. (2016), for an inferred distance modulus ($\mu_0 = 19.0 \pm 0.1$ mag) in excellent agreement with the values quoted above.

6 SUMMARY AND FUTURE PERSPECTIVES

We have presented the multiwavelength optical and NIR light-curve model fitting for a sample of 12 Cepheids (nine fundamental and three FO pulsators) in the SMC, in order to constrain their instrinsic stellar parameters and distances. The optical photometry was taken from data of the OGLE collaboration, while the near-infrared photometry (*JK* filters) is based on VMC observations. For three stars, radial velocity curves were also available and the best-fitting model was obtained by combining photometric and radial velocity data.

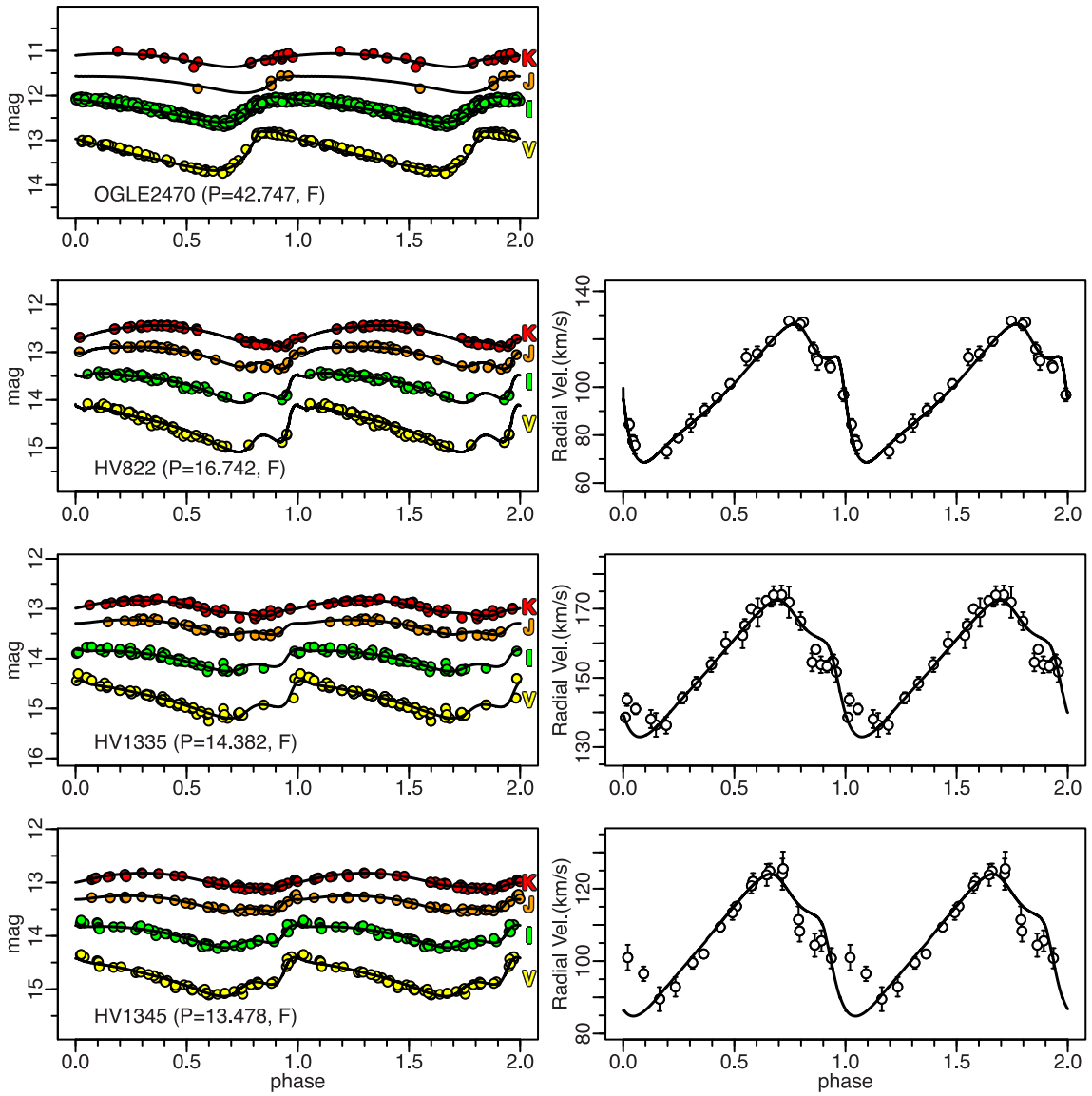

Figure 6. Model fitting of the photometric data of the longest period star OGLE2470 (left upper single panel) and of the selected SMC Cepheids for which multifilter light (left-hand panels) and radial velocity (right-hand panels) curves are available. The variable identification, pulsation period and mode are labelled in each panel. As the mean error bar for photometry is always <0.02 mag, we do not plot it for clarity reasons.

Following this approach, we were able to derive the intrinsic properties and the individual distances for the Cepheids in our sample, and in turn to find that:

(i) The intrinsic masses and luminosities of the inferred best-fitting models show that all these pulsators are brighter than the canonical evolutionary MLR suggesting a significant efficiency of core overshooting and/or mass-loss. Assuming that the inferred deviation from the canonical MLR is only due to mass-loss, we also discussed the distribution of the percentage mass-loss as a function of the pulsation period and the canonical stellar mass.

(ii) The inferred individual distances provide a mean value for the SMC distance modulus in agreement with the literature and a dispersion that can be ascribed to real variations in distance within the SMC. Indeed, there is evidence in the literature that the depth of the SMC is up to ∼0.3 mag (see e.g. Glatt et al. 2008; Subramanian & Subramaniam 2009, and references therein).

(iii) The obtained stellar radii can be correlated with the periods to build a PR relation that is found to be in excellent agreement with current PR relations derived in the literature for SMC Cepheids.

(iv) The absolute magnitudes of the best-fitting models were combined with the period information to show the behaviour of the investigated stars in the PL and Period–Wesenheit planes, finding an excellent agreement with published relations based on VMC data.

The results of this investigation support the predictive capabilities of the adopted theoretical scenario in terms of individual distances and intrinsic stellar parameters and pave the way for the application to other extensive data bases at various chemical compositions, including the VMC LMC pulsators (Ragosta et al., in preparation).

In the future, we also plan to extend the application to FO pulsators in order to better constrain their PL and Period–Wesenheit relations and to test the accuracy of the method through application to the light curves of Galactic CCs with *Gaia* parallaxes (Gaia

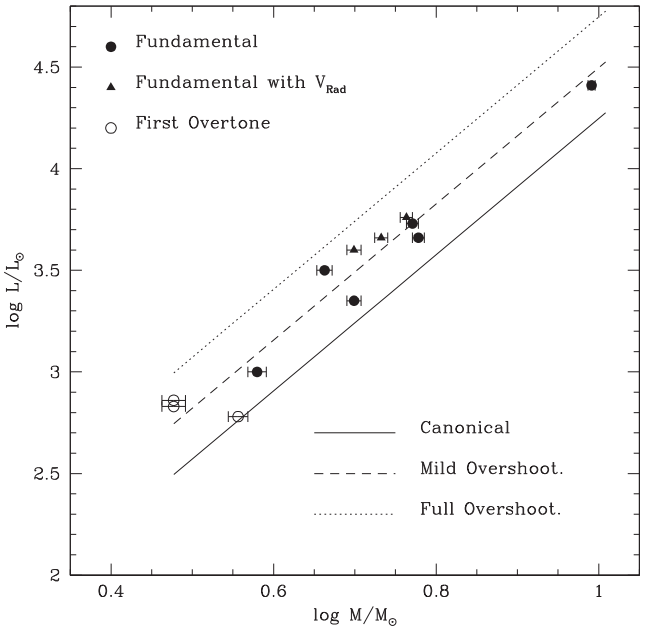

Figure 7. Predicted MLR based on the model fitting results for both F (black solid circles) and FO Cepheids (open circles). The best-fitting model location in the MLR plane is compared with an evolutionary MLR obtained by neglecting both mass-loss and core overshooting and labelled as 'Canonical' (solid line) and with the relations obtained by assuming mild (dashed line; corresponding to an extension of the extra-mixing region beyond the Schwarzschild border of about 0.2 H_p, where H_p is the pressure scaleheight) or full (dotted line) overshooting.

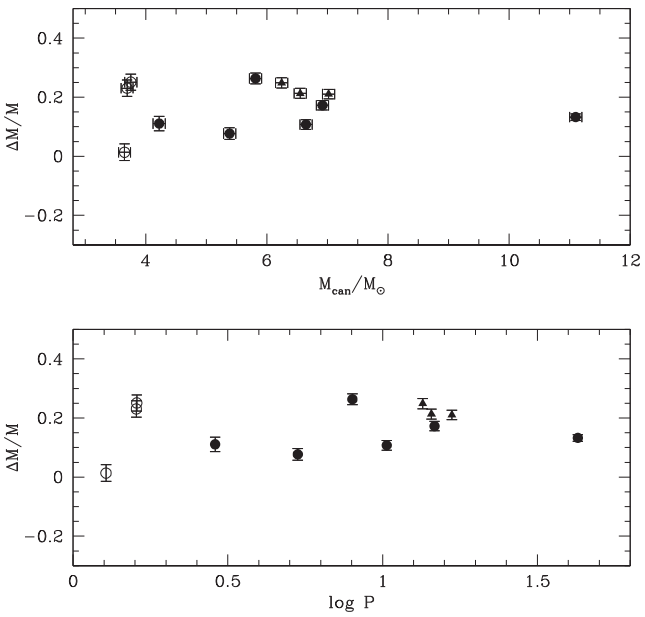

Figure 8. Predicted deviation of the best-fitting stellar mass from the value corresponding to the canonical M for both F (black solid circles) and FO Cepheids (open circles).

Collaboration et al. 2016; Gaia Collaboration 2016). The latter comparison, once the distance to the Gaia results is fixed, will also allow us to put strong constraints on the physical and numerical assumptions adopted in the hydrodynamical code as well as on the predicted stellar masses, MLR, and, provided that the metallicity is precisely

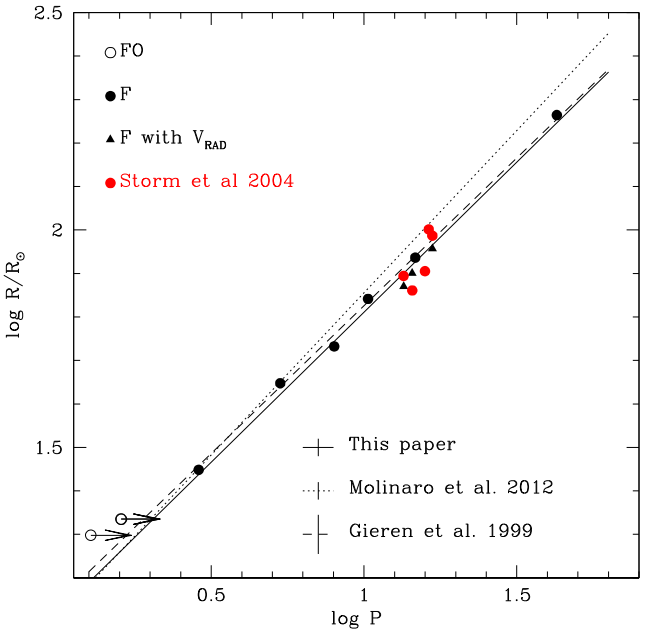

Figure 9. Predicted PR relation based on the model fitting results for both F (black solid circles) and FO Cepheids (open circles). The latter have been fundamentalized (see arrows) before performing the linear regression (solid line). The obtained PR has been compared with the location of SMC Cepheids with radius estimates by Storm et al. (2004) and with the relations by Molinaro et al. (2012, dotted line) and Gieren, Moffett & Barnes (1999, dashed line).

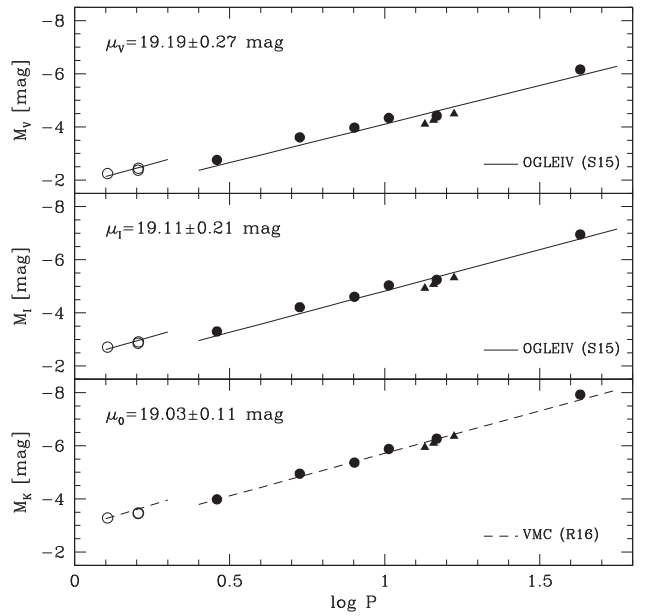

Figure 10. Predicted PL relation in the *V* (top panel), *I* (middle panel) and *K* (bottom panel) bands based on the model fitting results for both F (black solid circles) and FO (open circles) Cepheids. The empirical relations by the OGLE IV (solid lines) and VMC (dashed line) collaborations are shown for comparison and used in combination to the predicted absolute magnitudes to infer the labelled distance moduli.

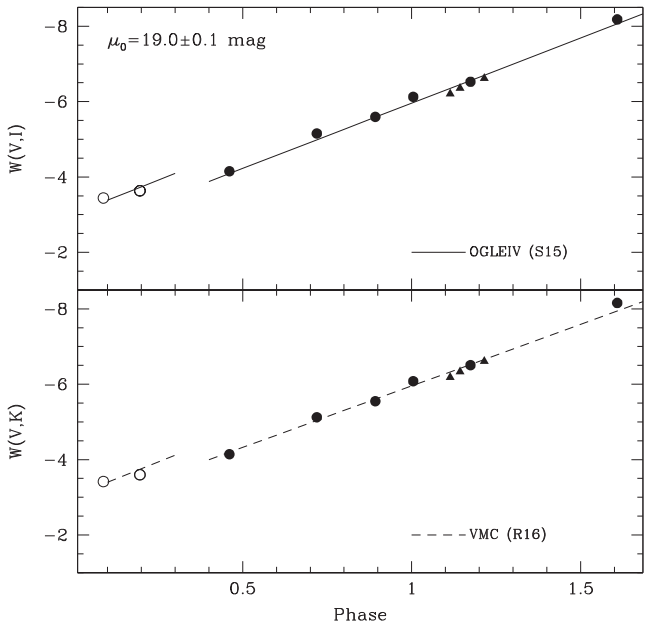

Figure 11. Predicted PW relations in the '*V*, *I*' (top panel) and '*V*, *K*' (bottom panel) filters for both F and FO pulsators, compared with the empirical relations by Soszyński et al. (2015) and Ripepi et al. (2016).

constrained by complementary spectroscopic data, on the helium to metal enrichment ratio.

ACKNOWLEDGEMENTS

We thank our referee, N. Nardetto, for his useful comments and suggestions. We also deeply thank J. P. Emerson for a critical reading of the paper and valuable comments. This work was supported by PRIN INAF 2014 (P.I.: Clementini). We thank the CASU and the Wide Field Astronomy Unit (WFAU) in Edinburgh for providing calibrated data products under the support of the Science and Technology Facility Council (STFC) in the UK. MRC acknowledges support from the UK's Science and Technology Facilities Council (grant number ST/M00108/1). RdG acknowledges research support from the National Natural Science Foundation of China (NSFC) through grants 11373010, 11633005 and U1631102. This project has received funding from the European Research Council (ERC) under the European Union's Horizon 2020 research and innovation programme (grant agreement no. 682115). Based on observations collected at the European Organization for Astronomical Research in the Southern hemisphere under ESO programme(s) 179.B-2003.

REFERENCES

Alcock C. et al., 1999, PASP, 111, 1539
Andersen M. I., Freyhammer L., Storm J., 1995, ESO Conf., 53, 87
Bessell M. S., Brett J. M., 1988, PASP, 100, 1134
Bono G., Marconi M., Stellingwerf R. F., 1999a, ApJS, 122, 167
Bono G., Caputo F., Castellani V., Marconi M., 1999b, ApJ, 512, 711
Bono G., Caputo F., Cassisi S., Marconi M., Piersanti L., Tornambé A., 2000, ApJ, 543, 955
Bono G., Gieren W. P., Marconi M., Fouqué P., Caputo F., 2001, ApJ, 563, 319
Bono G., Castellani V., Marconi M., 2002, ApJ, 565, L83
Bono G., Caputo F., Marconi M., Musella I., 2010, ApJ, 715, 277
Caputo F., Marconi M., Musella I., 2000, A&A, 354, 610
Caputo F., Bono G., Fiorentino G., Marconi M., Musella I., 2005, ApJ, 629, 1021
Castelli F., Gratton R. G., Kurucz R. L., 1997a, A&A, 318, 841
Castelli F., Gratton R. G., Kurucz R. L., 1997b, A&A, 324, 432
Carpenter J. M., 2001, AJ, 121, 2851
Cassisi S., Salaris M., 2011, ApJ, 728, L43
Chiosi C., Wood P. R., Capitanio N., 1993, ApJS, 86, 541
Christy R. F., 1970, J. R. Astron. Soc. Can., 64, 8
Cioni M.-R. L. et al., 2011, A&A, 527, A116
Dalton G. B. et al., 2006, in McLean I. S., Masanori I., eds, Proc. SPIE, Vol. 6269, Ground-based and Airborne Instrumentation for Astronomy. SPIE, Bellingham, 62690
de Grijs R., Bono G., 2015, AJ, 149, 179
Emerson J., McPherson A., Sutherland W., 2006, The Messenger, 126, 41
Fiorentino G., Musella I., Marconi M., 2013, MNRAS, 434, 2866
Freedman W. L. et al., 2001, ApJ, 553, 47
Fricke K., Stobie R. S., Strittmatter P. A., 1971, MNRAS, 154, 23
Gaia Collaboration et al., 2016, A&A, 595, A2
Gaia Collaboration et al., 2016, A&A, 595, A1
Gieren W. P., Moffett T. J., Barnes T. G., III, 1999, ApJ, 512, 553
Glatt K. et al., 2008, AJ, 136, 1703
Haschke R., Grebel E. K., Duffau S., 2011, AJ, 141, 158
Keller S. C., Wood P. R., 2006, ApJ, 642, 834
Luck R. E., Moffett T. J., Barnes T. G., III, Gieren W. P., 1998, AJ, 115, 605
McNamara D. H., Clementini G., Marconi M., 2007, AJ, 133, 2752
Madore B. F., 1982, ApJ, 253, 575
Madore B. F., Freedman W. L., 1991, PASP, 103, 933
Marconi M., Clementini G., 2005, AJ, 129, 2257
Marconi M., Musella I., Fiorentino G., 2005, ApJ, 632, 590
Marconi M., 2009, Mem. Soc. Astron. Ital., 80, 141
Marconi M., Molinaro R., Ripepi V., Musella I., Brocato E., 2013a, MNRAS, 428, 2185
Marconi M. et al., 2013b, ApJ, 768, L6
Molinaro R., Ripepi V., Marconi M., Bono G., Lub J., Pedicelli S., Pel J. W., 2011, MNRAS, 413, 942
Molinaro R. et al., 2012, ApJ, 748, 69
Moretti M. I. et al., 2014, MNRAS, 437, 2702
Moretti M. I. et al., 2016, MNRAS, 459, 1687
Muraveva T. et al., 2015, ApJ, 807, 127
Musella I. et al., 2016, MNRAS, 457, 3084
Nardetto N. et al., 2017, preprint (arXiv:1701.01589)
Natale G., Marconi M., Bono G., 2008, ApJ, 674, L93
Neilson H. R., Lester J. B., 2008, ApJ, 684, 569
Neilson H. R., Engle S. G., Guinan E. F., Bisol A. C., Butterworth N., 2016, ApJ, 824, 1
Prada Moroni P. G., Gennaro M., Bono G., Pietrzyński G., Gieren W., Pilecki B., Graczyk D., Thompson I. B., 2012, ApJ, 749, 108
Riess A. G. et al., 2016, ApJ, 826, 56
Ripepi V., Moretti M. I., Clementini G., Marconi M., Cioni M. R., Marquette J. B., Tisserand P., 2012, Ap&SS, 341, 51
Ripepi V. et al., 2012, MNRAS, 424, 1807
Ripepi V. et al., 2014, MNRAS, 437, 2307
Ripepi V. et al., 2015, MNRAS, 446, 3034
Ripepi V. et al., 2016, ApJS, 224, 21
Romaniello M. et al., 2008, A&A, 488, 731
Saha A., Sandage A., Tammann G. A., Sandage A., Tammann G. A., Dolphin A. E., Christensen J., Panagia N., Macchetto F. D., 2001, ApJ, 562, 314
Soszyński I. et al., 2010, Acta Astron., 60, 17
Soszyński I. et al., 2015, Acta Astron., 65, 297
Stobie R. S., 1969, MNRAS, 144, 511
Storm J., Carney B. W., Gieren W. P., Fouqué P., Freedman W. L., Madore B. F., Habgood M. J., 2004, A&A, 415, 521
Subramanian S., Subramaniam A., 2009, A&A, 496, 399
Udalski A., Soszynski I., Szymanski M., Kubiak M., Pietrzynski G., Wozniak P., Zebrun K., 1999, Acta Astron., 49, 223
Valle G., Marconi M., Degl'Innocenti S., Prada Moroni P. G., 2009, A&A, 507, 1541
Wood P. R. S. Arnold A., Sebo K. M., 1997, ApJ, 485, L25

This paper has been typeset from a TEX/LATEX file prepared by the author.